

A HRTEM study of defects in silver-doped galena

A. PRING

Department of Mineralogy, South Australian Museum, North Terrace, Adelaide,
South Australia 5000, Australia

AND

T. B. WILLIAMS*

C.S.I.R.O. Division of Materials Science and Technology, Locked Bag 33, Clayton,
Victoria 3168, Australia

Abstract

Synthetic Ag-doped PbS samples were Ar ion beam milled and examined by HRTEM. The silver was found to aggregate in inclusions which have no crystallographic relationship to the PbS host, rather than forming crystallographic defects. The Ag₂S inclusions are 500 Å in diameter or larger. The limit of Ag substitution into PbS in solid solution in the absence of Bi or Sb is less than 0.1 mol %. The ion beam milling process introduced a large number of small dislocations in both Ag-doped and pure PbS specimens. These dislocations are thought to be formed through coalescences of point defects.

KEYWORDS: galena, silver, HRTEM, ion beam milling.

Introduction

It has long been recognised that much of the silver content of so called 'argentiferous' galena exists in the form of inclusions of silver-bearing sulphosalts, such as freibergite or diaphorite, rather than in solid solution. Some silver is incorporated into the galena structure via coupled substitutions such as $2\text{Pb}^{2+} = \text{Ag}^+ + \text{Bi}^{3+}$ or the antimony equivalent. High-resolution transmission electron microscopy (HRTEM) is an ideal technique for studying the structural nature of 'argentiferous' galena. Recently Sharp and Buseck (1993) employed this technique to investigate the distribution of Ag and Sb in natural galena from La Paz and Zacatecas. In addition to observing coherent intergrowths between the galena host and inclusions of franckeite and diaphorite, they noted the occurrence of small plate-like defects similar in appearance to Guinier-Preston zones.

In this study we investigated the structural nature of the uncoupled substitution of Ag in galena, since excess concentrations of Ag over Bi

and Sb had been noted in natural and synthetic specimens (van Hook, 1960; Bloem, 1956; Bloem and Kröger, 1956). Synthetic Ag-doped galenas were prepared from very high purity chemicals in order to avoid ambiguity in the interpretation of the chemical nature of structural features.

Experimental

Specimens were prepared from elemental lead, silver and sulphur, of Specpure grade (99.999%). Appropriate weights of the three components were sealed into evacuated silica glass ampoules and heated at 600°C for 48 hrs. The sulphide charges were then ground and resealed in evacuated silica glass ampoules and heated to 1100°C, before slowly cooling to 800°C over 24 hrs and finally quenching to room temperature. The composition of the samples ranged from 100 mol% PbS to 97.5 mol% PbS: 2.5 mol% Ag₂S. In the initial stages of the study, samples were prepared for examination in the HRTEM by grinding under acetone in an agate mortar, and then dispersed on Cu grids coated with holey carbon support films. This method, however, did not yield crystal fragments

*Present address JASCO International Co. Ltd., 4-21 Sennin-cho 2-chome, Hachioji City 193, Japan

with sufficiently thin edges to permit structural imaging in the HRTEM, so subsequently specimens were prepared by Ar ion milling. The ion milled discs were examined in several different transmission microscopes including a JEOL 4000 and a JEOL 200CX. These instruments had theoretical point-to-point resolutions in the range 1.6–2.3 Å. The JEOL 200CX microscope was fitted with a detector for energy-dispersive X-ray analysis.

A series of image simulations was performed by the conventional multi-slice method (Goodman and Moodie, 1974). This established that at values of defocus near to the so-called Scherzer defocus (Scherzer, 1949) and for foil thicknesses less than 100 Å, the image contrast in the high-resolution images could be directly interpreted in terms of electron density; thus the black dots in the images represent Pb and S atoms (in the [100] projection of the structure the Pb and S atom positions are superimposed). All images presented in this paper were recorded at or near the Scherzer defocus.

Results

There was little change in the physical appearance of the samples with increasing Ag content. In the reflected light microscope rounded inclusions (> 30 µm in diameter) of Ag₂S were clearly visible in the more silver-rich samples (> 0.5 mol % Ag). In

addition to these, much smaller inclusions were observed by HRTEM. The inclusions are typically oval to circular in section. It is difficult to establish the size of these smaller inclusions, as in general at least part of the Ag₂S had been milled away, but they seem to have a minimum diameter of approximately 500 Å. Fig. 1 is a HRTEM lattice image taken down [100]_{PbS} showing part of an Ag₂S inclusion embedded in the PbS matrix. There is no apparent orientational relationship between the Ag₂S lattice and that of the PbS host; there are, however, Moiré fringe effects where the two crystals overlap in the image. Energy-dispersive X-ray analysis confirmed the composition of the Ag₂S inclusions. Analysis of the PbS matrix, recorded from regions near to, but not including the Ag₂S inclusions, showed up to approximately 0.3% Ag but no Ar (see discussion).

Another feature in the image are the three small platelet-like defects aligned along [010] (Fig. 1). Similar platelets were also noted by Sharp and Buseck (1993) in images of ion-thinned galena specimens (see Fig. 5 in Sharp and Buseck 1993) but not in crushed grain specimens, and they therefore concluded that the platelets are artifacts of ion thinning. While the platelets appear to be like chemical precipitates (Guinier-Preston zones), they are also present in ion milled specimens of pure synthetic PbS. Fig. 2 is an image at higher resolution from an Ag-doped galena containing a

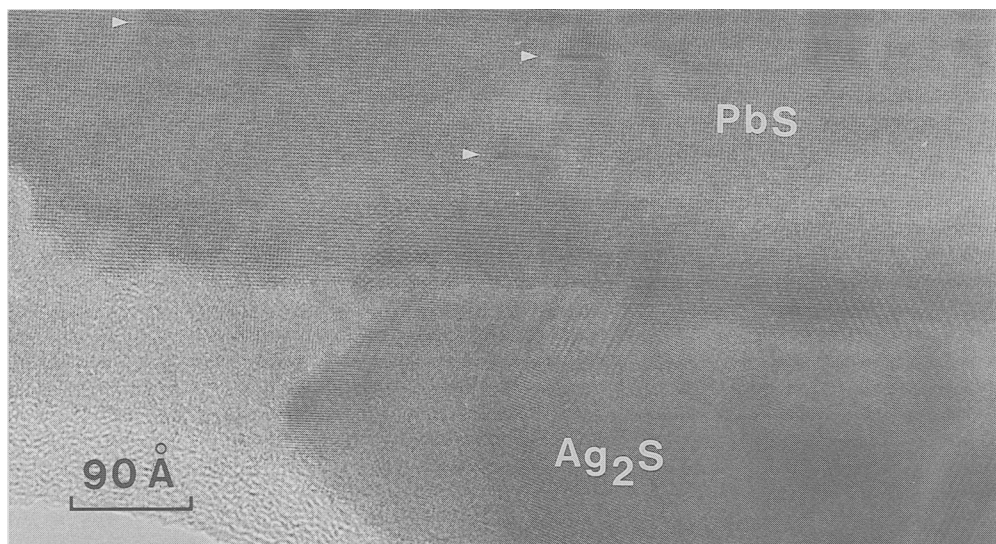


FIG. 1. Lattice image of PbS down [100] showing part of a Ag₂S inclusion. There is no orientational relationship between the PbS and Ag₂S lattices. The region where the two lattices overlap is dominated by Moiré fringes. Three small platelet-like defects are indicated in the PbS lattice. (JEOL 200CX).

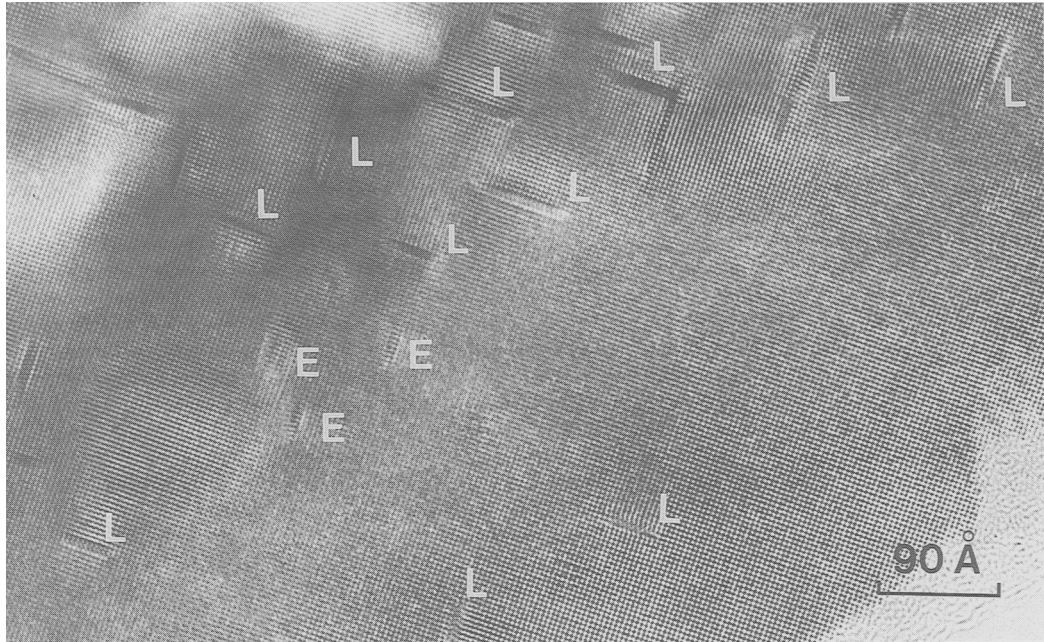


FIG. 2. High-resolution lattice image of platelets in Ag-doped PbS down [100]. Note that the platelets are aligned along [010] and [001] and they are surrounded by a strain field. The defects are one PbS cell wide and about 8 to 12 cells in length (~ 48 to 72 Å). Careful examination reveals that they are either terminations of edge dislocation (E) or sections through dislocation loops (L) (JEOL 4000).

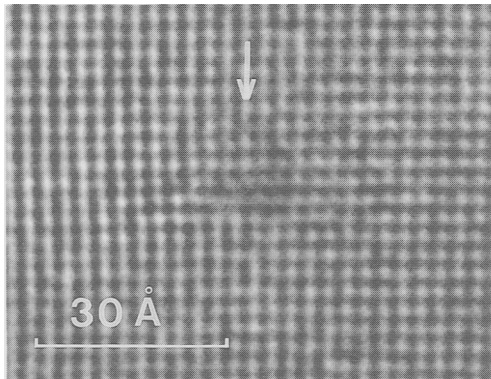


FIG. 3. Lattice image of PbS down [100] showing the termination of an edge dislocation with a Burgers vector $\frac{1}{2}[010]$. The extra half plane is indicated by an arrow. (JEOL 4000)

number of these platelets. They are aligned along the principle lattice directions [010] and [001]. The electron diffraction pattern from this part of the

crystal does not show streaking characteristic of Guinier-Preston zones (Patrick *et al.*, 1993) but rather, very faint and diffuse 100 reflections which are forbidden by the F type lattice. The defects appear to be one PbS unit cell wide (~ 6 Å) and range in length from about 8–12 unit cells (~ 48 – 72 Å) and are surrounded by a strain field. The platelets are much less common at the edge of the crystal. This suggests that they are three-dimensional features which need not penetrate through the thickness of the foil. There is also a distinct difference in the apparent length of the defects; they are longer in the thicker parts of the crystal indicating that they intersect the foil at an angle. Fig. 3 shows a defect from near the thin edge of the foil; it is clearly the termination of an edge dislocation with a Burgers vector $\frac{1}{2}[010]$. The defect shown in Fig. 4a, also from near the edge of the foil, represents the front view of the half-loop of a dislocation loop with a Burgers vector also $\frac{1}{2}[010]$. The atomic arrangement is shown diagrammatically in Fig. 4b. This section of crystal is probably less than 25 Å or so thick and the two extra half planes and the slip of the 6 planes across the line of the defect can be clearly

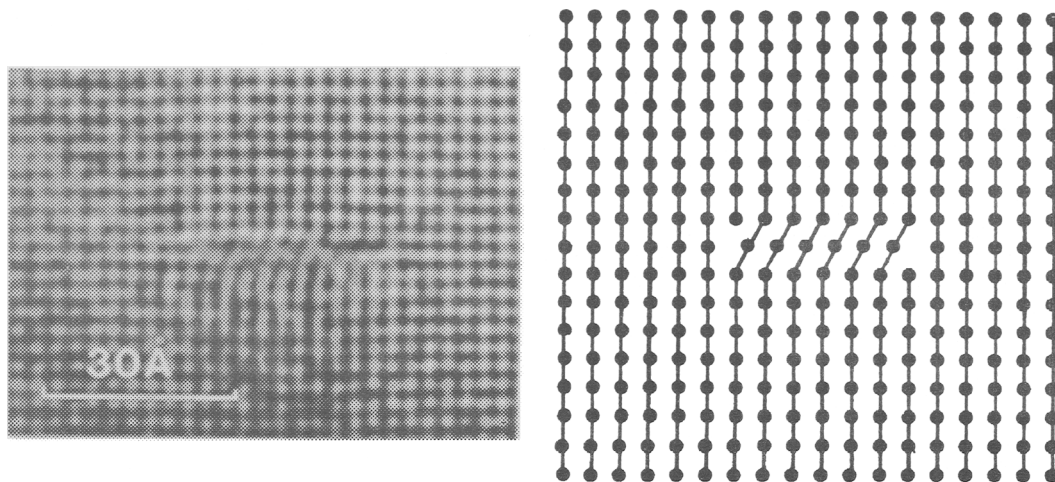


FIG. 4. (a, left) Lattice image of PbS down [100] showing a section through a dislocation loop. The slipped section of the lattice is six (200) planes wide. The Burgers vector for the dislocation is $\frac{1}{2}[010]$. Kinking of the lattice rows parallel to the slip is evident in the strain field associated with the dislocation. (JEOL 4000). (b, right) Schematic diagram showing the atomic arrangement in cross section of the dislocation loop.

traced. Note also that the planes of atoms around the defects are displaced, resulting in a strain field. Careful examination of the platelets in the thicker region of the crystal shown in Fig. 2 reveals that all defects are either terminations of edge dislocations or sections through screw dislocations. In this study no lattice defects which could be interpreted as clusters or precipitates of Ag atoms were observed.

Discussion

It is clear that most of the silver in the doped PbS specimens in this study is not incorporated into the PbS lattice but occurs as Ag_2S inclusions. In addition to the optically visible inclusions, suboptical inclusions of silver sulphide around 500 Å in diameter also occur. There is no apparent crystallographic orientation with respect to the host PbS lattice. Energy-dispersive X-ray analysis of the PbS host is inconclusive with respect to the presence of Ag in solid solution. Some analyses showed about 0.3 wt.% Ag; however this value is probably not significant due to the relatively poor detection limit for this type of *in situ* analysis, estimated at 0.2%, and to the presence of the Ag_2S inclusions elsewhere in the sample which may also emit X-rays due to the interaction of stray electrons. It is apparent however that only very small amounts of Ag can substitute into PbS without the additional presence of counter-atoms

such as Bi or Sb. The work of Bloem (Bloem, 1956; Bloem and Kröger, 1956) showed that a limited amount of non-stoichiometry is possible in the PbS structure (less than 0.1% deficiency of either Pb or S) and he showed that an S deficiency could be compensated for by Ag doping. Boorman (1968) suggested that the upper limit for Ag substitution in solid solution in natural PbS without the presence of the counter ions Bi or Sb is probably less than 0.1 mol %. The results of the present study are thus consistent with this figure.

This study also shows that argon ion milled PbS specimens contain many small dislocations. Argon ion milling with a high accelerating potential (>3 kV) can transform the galena crystal lattice to a mass of microcrystallites but much of this damage can be removed by further milling the sample with an Ar ion beam of 1 kV; the dislocations remain however. Attempts were made to remove the dislocations by the iodine ion mill method of Chew and Cullis (1984) but this process leads to a surface growth of PbI_2 crystals rather than producing electron transparent foils of PbS.

It is possible that some of the dislocations were introduced during cleaving of the original specimens. Zheng *et al.* (1988) suggested that edge dislocations can be introduced into PbS during the process of cleaving a crystal. They observed by STM a number of dislocations with a common orientation and Burgers vector intersecting the

cleavage surfaces of PbS. The dislocations found in the present work show two perpendicular orientations so could not have all been introduced during cleaving. Sharp and Buseck (1993) did not find any dislocation terminations in their crushed grain preparations and from this it can be concluded that most of the dislocations reported here were introduced by Ar ion milling. The process of ion beam milling may induce the formation of point defects through the loss of S. These vacancies may diffuse through the lattice under the action of the ion beam and coalesce, locally, to form small dislocations.

Acknowledgements

We wish to thank the following people for giving us access to the transmission electron microscopes in their charge: Dr D. A. Jefferson, Department of Chemistry, University of Cambridge, and Dr A. Spargo, Department of Physics, University of Melbourne. The practical assistance of Dr David Jefferson and Dr Tim White is greatly appreciated. The financial assistance of the Australian Research Council to A. P. is gratefully acknowledged.

References

Bloem, J. (1956) Controlled conductivity in lead sulphide single crystals. *Philips Research Reports*, **11**, 273–336.

- Bloem, J. and Kröger, F. A. (1956) The *P-T-X* phase diagram of the lead-sulphur system. *Z. physik. Chem., Neue Folge*, **7**, 1–14.
- Boorman, R. S. (1968) Silver in some New Brunswick galenas. New Brunswick Research and Productivity Council, Research Note 11.
- Chew, N. G. and Cullis A. G. (1984) Iodine ion milling of indium-containing compound semiconductors. *App. Phys. Lett.*, **44**, 142–4.
- Goodman, P. and Moodie A. F. (1974) Numerical Evaluation of N-beam wave functions in electron scattering by the multi-slice method. *Acta Cryst.*, **A30**, 280–90.
- Patrick, R. A. D., Dorling, M. and Polya, D. A. (1993) TEM study of indium- and copper-bearing growth-banded sphalerite. *Can. Mineral.*, **31**, 105–17.
- Scherzer, O. (1949) The theoretical resolution limit of electron microscopes. *J. Appl. Phys.*, **20**, 20–29.
- Sharp, T. G. and Buseck P. R. (1993) The distribution of Ag and Sb in galena: Inclusions versus solid solution. *Amer. Mineral.*, **78**, 85–95.
- van Hook, H. J. (1960) The ternary system $\text{Ag}_2\text{S}-\text{Bi}_2\text{S}_3-\text{PbS}$. *Econ. Geol.*, **55**, 759–88.
- Zheng, N. J., Wilson, I. H., Knipping, U., Burt, D. M., Krinsley, D. H. and Tsong, I. S. T. (1988) Atomically resolved scanning tunnelling microscopy images of dislocations. *Phys. Rev.*, **B38**, 12780–82.

[Manuscript received 15 February 1993:
revised 1 December 1993]